Available online at www.sciencedirect.com

ScienceDirect

Ceramics International 40 (2014) 2901–2914

CERAMICS INTERNATIONAL

www.elsevier.com/locate/ceramint

Behavior and mechanism of the stress buffer effect of the inside ceramic layer to the top ceramic layer in a double-ceramic-layer thermal barrier coating

Meng Han, Jihua Huang*, Shuhai Chen

School of Materials Science and Engineering, University of Science and Technology Beijing, Beijing 100083, China

Received 22 September 2013; received in revised form 22 September 2013; accepted 4 October 2013
Available online 18 October 2013

Abstract

The Double-Ceramic-Layer Thermal Barrier Coating (DCL-TBC) consists of a top ceramic layer (TC1), an inside ceramic layer (TC2), bond coat (BC) and alloy substrate. The top ceramic layer is made by new ceramic materials which has the lower thermal conductivity, such as LZ, LZ_7C_3, LMA etc. Although these materials have good high temperature performance and thermal insulation properties, their thermal expansion coefficients are very low which cause higher degree of mismatch with material properties of alloy substrate.

The behavior of the stress buffer effect of the layer of TC2 is investigated aiming at the DCL-TBC with the two ceramic layers as LZ_7C_3(TC1) and 8YSZ(TC2). A FE model of the DCL-TBC is established and the stress of the TC1 during the thermal cycles is calculated. Results show that the layer of TC2 has the behaviors of stress buffer effect on reducing the stress of TC1 and reducing the influence of the TGO growth upon the stress of TC1. The inner mechanism of the stress buffer effect is investigated based on the influence of the thermal expansion coefficient ρ of the TC2 layer. Results show that the TC1 layer varies with the TC2 layer, having different thermal expansion coefficients; and the stress buffer effect is dominant, affected by the thermal expansion coefficients of the TC2 layer. The thermal expansion coefficient should be neither too large nor too low; if its values are too low or too large, the stress levels of TC1 are all high. The reasonable range of the thermal expansion coefficient is investigated. Aiming at the DCL-TBC with the two ceramic layer thicknesses as 150 μm, the reasonable range of the thermal expansion coefficient of TC2 is from 10.35 $°C^{-1}$ ($\times 10^{-6}$) to 10.887 $°C^{-1}$ ($\times 10^{-6}$).

Keywords: The DCL-TBC; The stress buffer effect; FE numerical simulation; The reasonable range of the thermal expansion coefficient

1. Introduction

The rapid development of aeronautical technology puts forward a higher requirement for aero engine performance, such as the performances of high flow ratio, high thrust-weight ratio, high turbine inlet temperature and especially the performances of high temperature resistant of combustion chamber. Thermal barrier coatings (TBC) have been widely used as an effective measure to improve high temperature resistance of hot components in the aircraft engine. The typical TBC used in gas turbines consists of a bond coat MCrAlY (M=Ni, Co) and a top coat of 8YSZ. But, at the temperature higher than 1200 °C, phase transformation and sintering will happen in YSZ which are the major disadvantages of YSZ. It will cause large stress level during the service process. In this case, the service life is greatly reduced which is difficult to meet the further requirements of high performance aero engine.

To overcome the disadvantages of YSZ, the search of candidate materials that can withstand higher gas-inlet temperature has been intensified in the past. Since the materials with the physical properties such as lower thermal conductivity than YSZ and high thermal stability up to its melting point were proposed as the promising materials, such as lanthanum zirconate (LZ), cerium lanthanum zirconate (LZ_7C_3), $LaMgAl_{11}O_{19}$ (LMA), etc. However, with good high temperature performance and thermal insulation properties, these new thermal insulation materials have very low thermal expansion

*Corresponding author. Tel.: +86 1062334859.
E-mail address: 569387571@qq.com (J. Huang).

0272-8842/$ - see front matter © 2013 Elsevier Ltd and Techna Group S.r.l. All rights reserved.
http://dx.doi.org/10.1016/j.ceramint.2013.10.021

coefficients which cause higher degree mismatch with material properties of alloy substrate. In this case, the stress level of the ceramic layer is usually very high and the cycle life is also very low [1]. So the traditional two-layer structure of thermal barrier coating, which is made by the ceramic layer and bond coat layer, cannot satisfy the requirement of the aeronautical technology development, it is necessary to explore new structures of the TBCs.

Based on the multilayer system, Double-Ceramic-Layer Thermal Barrier Coating turns out to be an effective method to meet the demands of development of thermal barrier coatings [1,2]. The Double-Ceramic-Layer Thermal Barrier Coating (DCL-TBC) includes a top ceramic layer (TC1), an inside ceramic layer (TC2), bond coat (BC) and alloy substrate (SUB). The top ceramic layer is made by new ceramic materials which have lower thermal conductivity, such as LZ, LZ_7C_3 and LMA mentioned above. The inside ceramic layer is usually made by the traditional materials, such as 8YSZ, which have the larger thermal expansion coefficient and good tolerance.

At present, the researches of the DCL-TBC are mainly based on experiments. As reported by Cao [3,4], the thermal cycling of the DCL-TBC LZ_7C_3/8YSZ has an excellent performance and a longer thermal cycling lifetime compared with single ceramic layer coatings. The good insulation performance is determined by the top ceramic layer, as the material of which has lower thermal conductivity. The traditional thermal barrier coatings, which are made by one ceramic layer, had been studied for many years. It had been concluded that the damages and failure behavior in the TBC are related to the residual stress under the thermo-mechanical loading [3–7]. And for the DCL-TBC studied in the present paper, it had been discussed that, if the coating system has no inside ceramic layer, the top ceramic layer usually has higher stress level, as the materials of the TC1 layer usually have lower thermal expansion coefficient which causes high degree thermal expansion mismatch between the top ceramic layer and the BC or SUB layer. In that case, the TC2 layer is introduced in the DCL-TBC as a stress buffer layer for the main purpose of ensuring that the stress of TC1 can be reduced in a lower level. This stress buffer effect of the inside ceramic layer has only been concluded through the experiment researches. Refer to results reported by Cao, the DCL-TBC LZ_7C_3/8YSZ has much longer thermal cycling life compared with the traditional LZ_7C_3 single-Ceramic-Layer TBC. It can be concluded that the high stress level of LZ_7C_3 layer (the TC1 layer) has been improved by introducing the 8YSZ as the inside ceramic layer [3,4]. But the explanation of this buffer effect using the stress theory has not been reported.

Based on these considerations, the first key issue of the present paper was to investigate the behaviors of stress buffer effect of the TC2 layer on stress distribution of TC1 in the DCL-TBC. In our study, a numerical model has been developed to assess the thermo-mechanical behavior of the DCL-TBC system using the finite element code ANSYS. Important parameters such as the interface roughness at the TC1/TC2 and TC2/BC, the cyclic loading, the volume growth of the TGO, the creep relaxation and plastic deformation are taken into account to predict their effects upon the stress distribution of the DCL-TBC system.

For the further study, the influence of the thermal expansion coefficient ρ of the TC2 layer upon the stress of the TC1 layer was investigated to discuss the inner mechanism of the stress buffer effect. Calculation results show that the stress of the TC1 layer is different as the TC2 layer has different values of ρ. Especially, if the thermal expansion coefficient of the TC2 layer is too large or too low, the stress level of TC1 is still high and the TC2 layer has little stress buffer effect. The ρ of the materials chosen for the TC2 layer should have a reasonable range: if the thermal expansion coefficient ρ of the TC2 layer is in this range, the stress level of TC1 layer can be in a safe state and the stress buffer effect of the TC2 layer is effective. Based upon these considerations, the stress safety criterion of the TC1 layer was proposed based on the theories of the fracture mechanics, and the reasonable range of the ρ of TC2 was discussed. This work has revealed the inner influence mechanism of the stress buffer effect of the TC2 layer. The reasonable range of the thermal expansion coefficient of the TC2 layer shows the basic condition of the material for the inside ceramic layer, and can provide guidance to the material selection of the TC2 layer for the DCL-TBC.

It should be mentioned that all the works are aiming at the DCL-TBC in which the top ceramic layer is made by LZ_7C_3 and the thicknesses of the two ceramic layers are 150 μm. The reasonable range of the ρ of TC2 in the DCL-TBC with different top ceramic layers or different ceramic layer thickness ratios can also be discussed using the same method and is not detailed in the present paper, as the main purpose of the present paper is to provide the method.

2. The simulation scheme

2.1. The numerical model, boundary conditions and thermal cycle load

Fig. 1 illustrates the schematic view of the numerical model. Based on the structure of the DCL-TBC, the numerical model is made of the top ceramic layer (TC1), the inside ceramic layer (TC2), thermally grown oxide layer (TGO), bond coat (BC) and substrate layer (SUB). The thicknesses of BC and substrate were 50 μm and 1500 μm. The initial TGO thickness was set to 1 μm and the TGO thickness varied between values of 1 μm to 5 μm during the thermal cycling. The thickness of TC1 (H_{TC1}) was 150 μm and the thickness of TC2 (H_{TC2}) was set as variable for studying the influence of the thickness upon stress buffer effect.

The model was meshed with 2-D 4-Node elements (ANSYS10.0 PLANE182 element) with generalized plane strain. The geometries of the TC1/TC2 and TGO interface were taken to be a semicircle wave to simulate surface roughness conditions typical for plasma sprayed TBCs [5–8]. In our work, the wavelength and amplitude of the semicircle were all set to 15 μm, i.e. R=15 μm. The FE model was

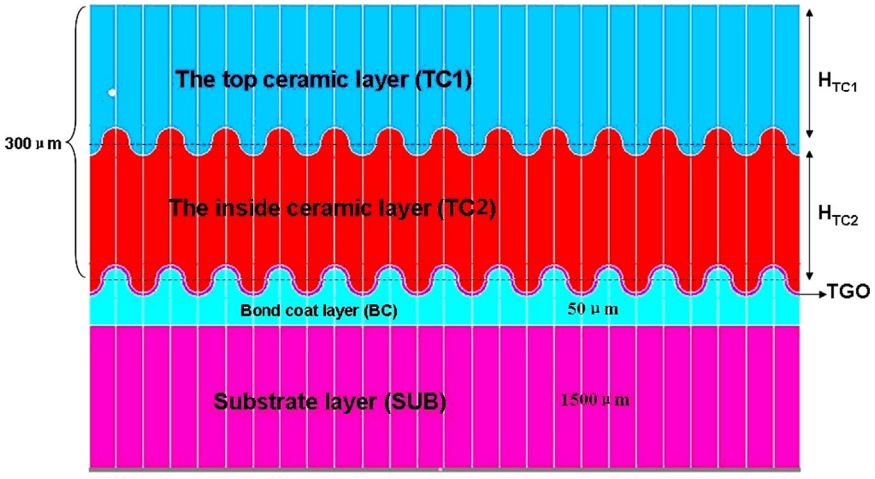

Fig. 1. The schematic view of the numerical model.

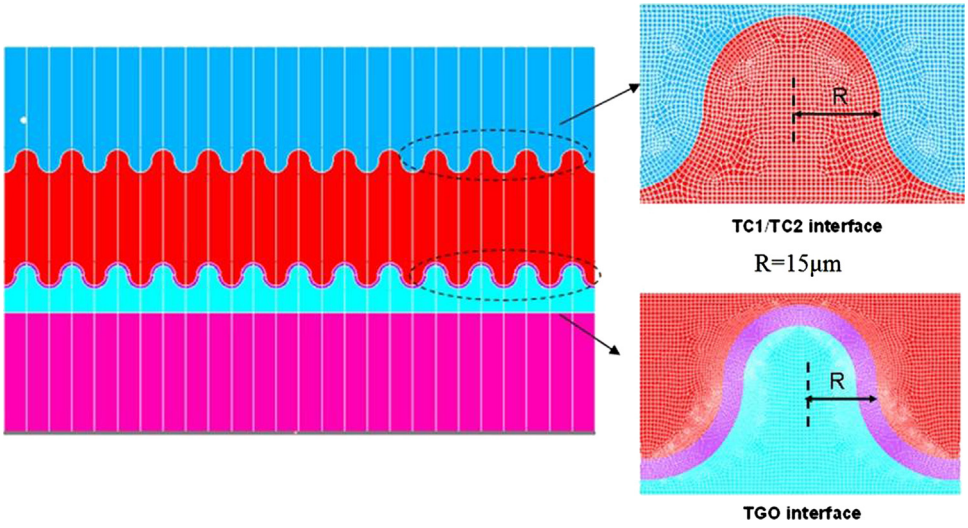

Fig. 2. Meshing applied to the two interfaces in the DCL-TBC.

performed using different mesh sizes, as the parts in the interface were meshed fine (Fig. 2).

2.2. Thermal cycle load

The thermal loads in model consisted of high temperature heat source and low temperature heat source as shown in Fig. 3. For the case of a single cycle, the load consisted of four steps. First, heating from 25 °C to 1300 °C at high temperature heat source (25–1000 °C at low temperature heat source) in 15 min, followed by a dwell-time at 1300 °C at high temperature heat source (1000 °C at low temperature heat source) for 10 h. Cooling from 1300 °C to 25 °C (1100 °C to 25 °C) also took 15 min. As a last step a holding time at low temperature (25 °C) of 15 min was introduced. At dwell stage at high temperature, TGO layer was modeled as growing.

2.3. Boundary conditions and the initial stress-free state

Regarding a Cartesian coordinate system, the displacement in *X*-direction of the nodes lying on the left edge of the segment and the displacement in *Y*-direction of the nodes lying on the bottom edge of the segment had been constrained, as shown in Fig. 4.

The value of temperature equal to 200 °C was chosen for the initial stress-free state for all layers [5]. It matches approximately with the coating stress-free temperature for the air plasma spraying process. At this temperature, each layer has begun to restrict each other after spraying.

2.4. The method of numerical simulation

As proposed in Fig. 4, the model consisted of lots of "sub-model" in horizontal (*X*) direction. Each sub-model included a complete cycle of roughness. On the basis of boundary conditions, the model was investigated in three sub-model parts named "the right edge", "the central" and "the left end" (respectively denoted by "Part I", "Part II" and "Part III" in Fig. 4). The three parts represent three kinds of states in actual DCL-TBC. Specifically, "the right edge" represents the coating located in the actual edge, "the left end" represents the coating away from the actual edge and "the central" represents the

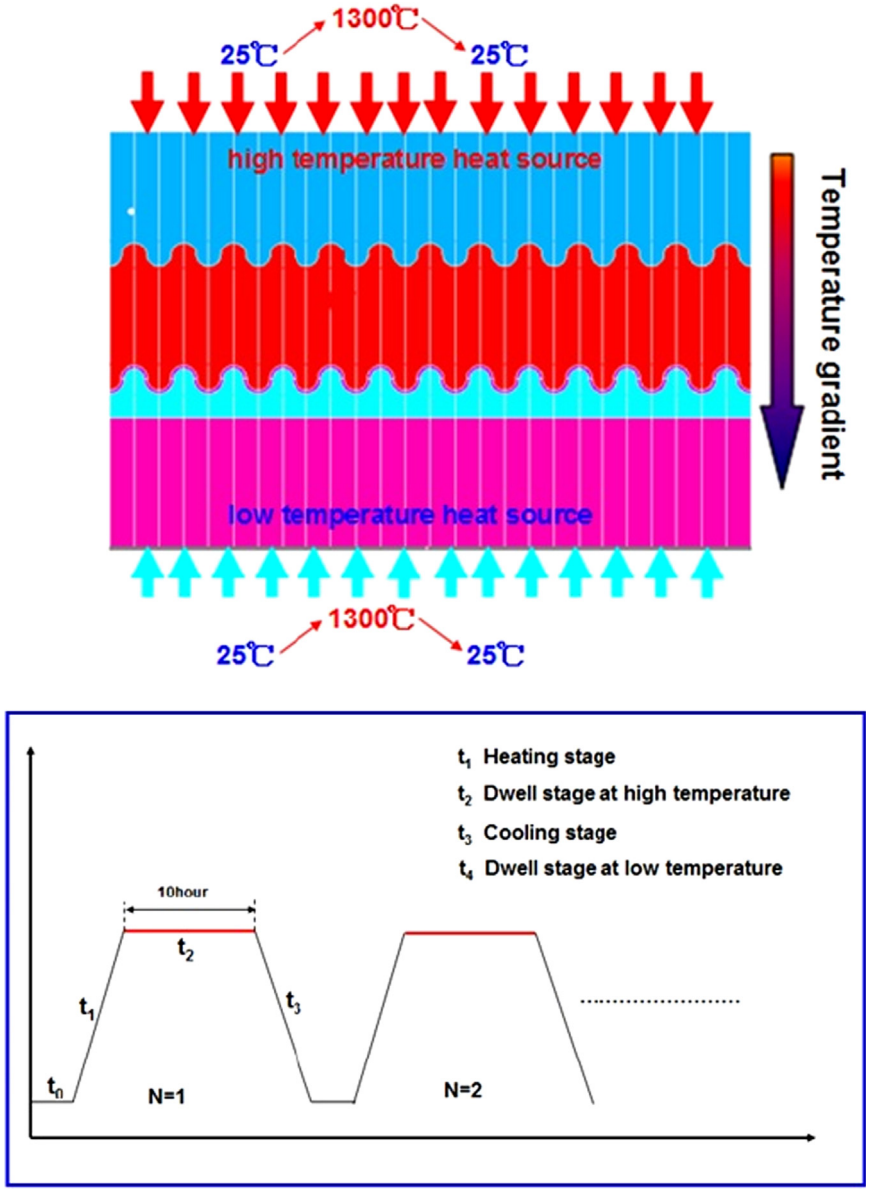

Fig. 3. Thermal cycle used in FEM simulation: thermal loads and steps in a single cycle.

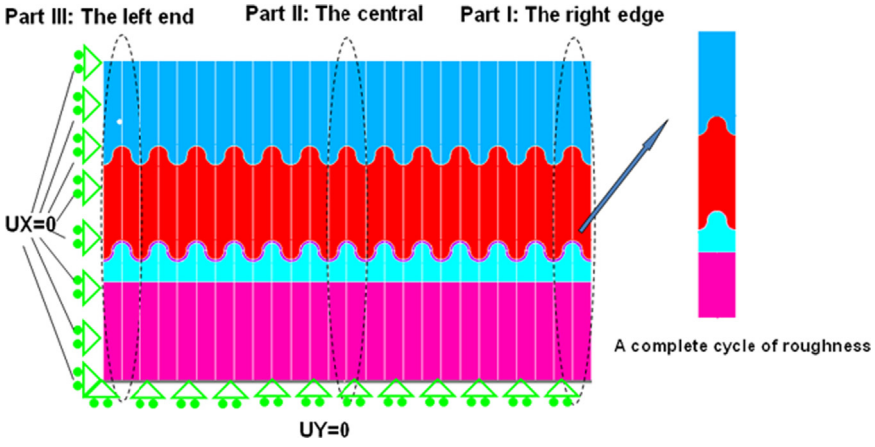

Fig. 4. The three parts in study and the boundary conditions of model.

Table 1
Material parameters of 8YSZ [13].

T (°C)	20	200	500	700	1100	1400	T (°C)	20
E (GPa)	48	47	43	39	25	15	λ (W m^{-1} k^{-1})	1.8
γ	0.1	0.1	0.1	0.11	0.12	0.12	C (J Kg^{-1} K)	640
α (10^{-6} K^{-1})	10.4	10.5	10.7	10.8	10.9	11.3	ρ (Kg m^{-3})	5.28e3

Table 2
Material parameters of BC (NiCoAlY) [10].

T (°C)	20	200	600	800	1000	1100	T (°C)	20
E (GPa)	152.4	143.3	133.3	117.9	74.16	41.07	λ (W m^{-1} k^{-1})	15
γ	0.311	0.320	0.338	0.345	0.351	0.354	C (J/Kg K)	628
α (10^{-6} K^{-1})	12.3	13.2	15.2	16.3	17.2	17.7	ρ (Kg m^{-3})	7.80e3

Table 3
Material parameters of TGO [10].

T(°C)	20	200	800	1000	1100	1400	T(°C)	20
E (GPa)	400	390	355	325	315	310	λ (W m^{-1} k^{-1})	5.8
γ	0.23	0.23	0.25	0.25	0.25	0.26	C (J Kg^{-1} K)	600
α (10^{-6} K^{-1})	7.13	7.47	9.0	9.5	9.7	9.8	ρ (Kg m^{-3})	4.20e3

Table 4
Material parameters of LZ_7C_3 (top ceramic layer).

T (°C)	20	400	800	1200	T (°C)	20
E (GPa)	175	167	150	135	λ (W m^{-1} k^{-1})	0.5
γ	0.2	0.2	0.2	0.2	C (J Kg^{-1} K)	490
α (10^{-6} K^{-1})	9.1	8.51	9.1	9.1	ρ (Kg m^{-3})	4.59e3

transitional regions between “the right edge” and “the left end”. In our study, stress buffer effect of the TC2 had been investigated in three parts as represented with consideration to the influence of the edge stress concentration.

In order to make ensure that the meshing of different cycles was consistent, one part of cycle was meshed firstly, and then copied by parallel movement to be a complete meshing.

2.5. Material behavior

All layers are homogeneous and isotropic. The thermally grown oxide and the two ceramic layers are treated as elastic and viscous materials. The bond coat is treated as plastic and viscous materials. Concerning the recent works of Bialas, the results show that the effects of plastic and creep of substrate to the stress level of coating system are very small [5]. Based on his result, the substrate is treated as an elastic material. The material parameters of TC1 (LZ_7C_3) are based on the experiment measurement. The mechanical properties of all the layers are functions of temperature as listed in Tables 1–7.

2.5.1. The investigation of material property ρ of TC2

For the first key issue of the present paper, which is the investigation of the behavior of stress buffer effect, the TC2 layer was aiming at the material of 8YSZ which is widely used as the inside ceramic layer in the DCL-TBC. The material parameters of 8YSZ are listed in Table 1.

For the second issue, the investigation, which is the influence of material property upon the stress buffer effect, was mainly focused on the thermal expansion coefficient ρ. The values of ρ investigated were selected from 9.4 °C^{-1} ($\times 10^{-6}$) to 12.8 °C^{-1} ($\times 10^{-6}$), and other material parameters were the same as the material parameters of 8YSZ which is listed in Table 1.

2.5.2. Creep

The creep properties strongly depend on the temperature. Their effects will be important when the system is at temperatures higher than approximately 600 °C as mentioned by Pan et al. [9]. For all layers, the following Norton power-law creep

Table 5
Material parameters of SUB [10].

T(°C)	20	200	400	600	800	1000	T (°C)	20
E (GPa)	220	210	190	170	155	130	λ (W m^{-1} k^{-1})	20
γ	0.31	0.32	0.33	0.33	0.34	0.35	C (J Kg^{-1} K)	658
α (10^{-6} K^{-1})	14.8	15.2	15.6	16.2	16.9	17.5	ρ (Kg m^{-3})	8.15e3

(2) Nonlinear parameters.

Table 6
Plastic parameters of BC [8].

Stress (MPa)	Plastic strain	T (°C)
1000	0	25
2500	0.23	400
2200	0.3	600
375	0.022	800
60	0.02	900
19	0.01	1000

Table 7
Creep parameters of all layers.

	B (s^{-1} MPa^{-n})	n	T (°C)
TC2 [11]	1.8(10^{-11}–10^{-5})	1	1000
TGO [7]	7.3(10^{-12}–10^{-4})	1	1000
BC [8]	6.54E^{-19}	4.57	≤600
	2.20E^{-12}	2.99	700
	1.84E^{-7}	1.55	800
	2.15^{-8}	2.45	≥850

behave is used:

$$\dot{\varepsilon}_{cr} = B\sigma^n \quad (1)$$

Where $\dot{\varepsilon}_{cr}$ is the strain rate (s^{-1}), B is the pre-factor (s^{-1} Mpa^{-n}), σ is the stress (Mpa) and n is the power-law creep exponent. The coefficients of B and n are also temperature dependent as listed in Table 7.

2.5.3. TGO growth

At the dwell-time in the thermal cycle, the TGO is growing at high temperature. Oxidation kinetics had been identified in isothermal oxidation experiments and fitted to Eq. (2) by Hermosilla [12].

$$H_{tgo} = K_{p0}\sqrt{t}\ K_{p0} = \exp\left(Q\left(\frac{1}{T_0} - \frac{1}{T}\right)\right)\ (\mu m/\sqrt{s}) \quad (2)$$

the parameter t denotes the total time of oxidation, Q and T_0 are experimentally determined constants. According to the results of oxidation test, the two constants were determined as Q=27777.4 K and T_0=2721 K. In order to study the stress buffer effect independently, the oxidation temperature was chosen as 1100 °C without considering the influence of different thickness ratios of two ceramic layers.

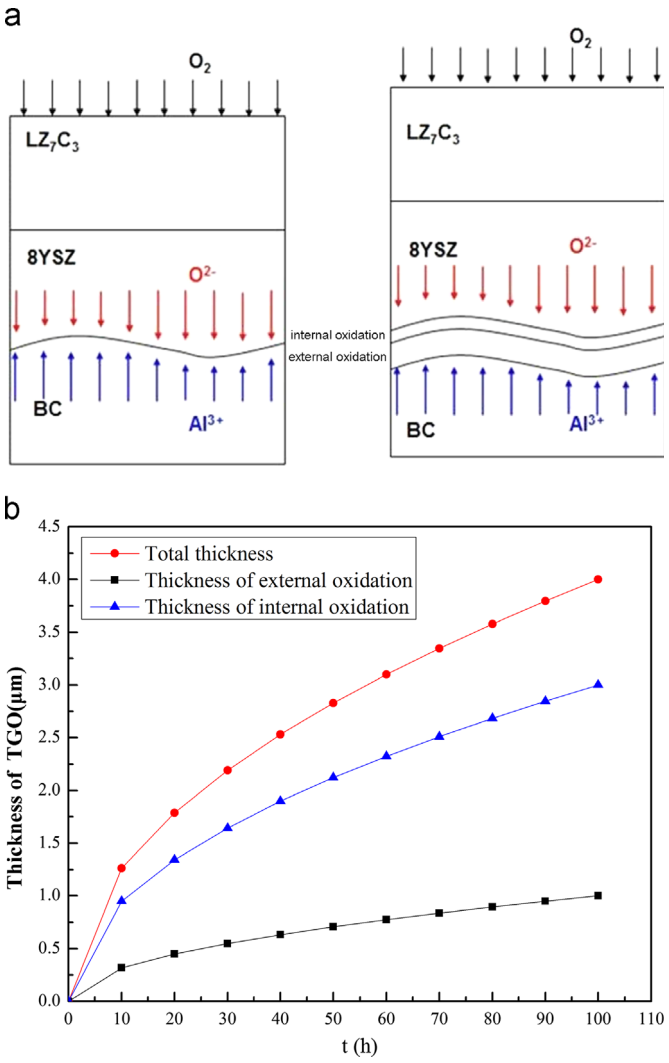

Fig. 5. Schematic representation of the internal and external oxidation processes: (a) internal and external diffusion and (b) the TGO growth curves in study.

Based on studies of the other authors, the thickness of TGO was divided into the thickness of internal oxidation (h_1) and external oxidation (h_2) in our study and the ratio between h_1 and h_2 is defined as 3 [12–15]. The curves of TGO growth are show in Fig. 5(b) (total thickness h_0; thickness of internal oxidation h_1 and external oxidation h_2).

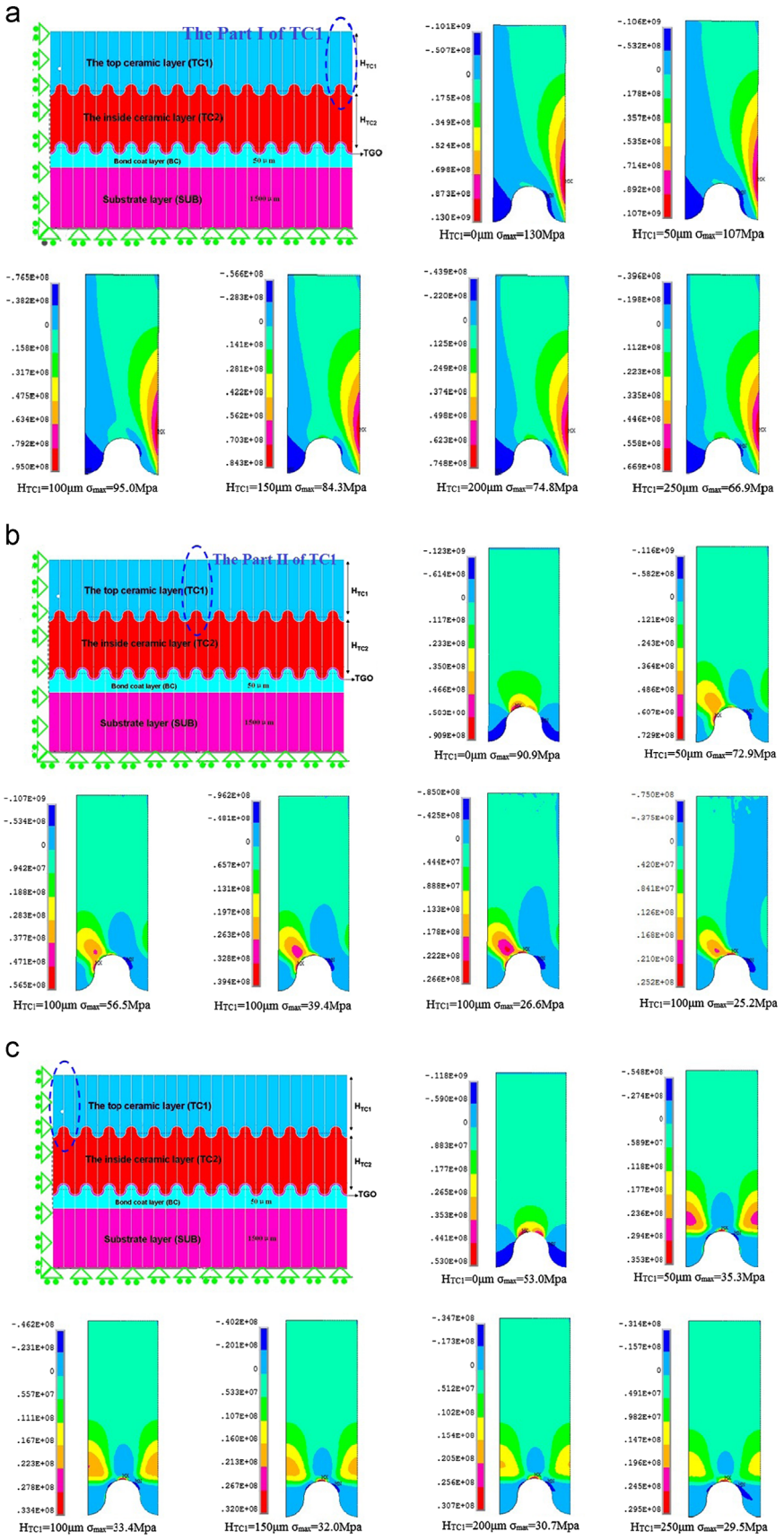

Fig. 6. The stress cloud charts of the TC1 with the thicknesses of TC2 as 0 μm, 50 μm, 100 μm, 150 μm, 200 μm and 250 μm: (a) the Part I in TC1, (b) the Part II in TC1, (c) the Part III in TC1. (a) The stress cloud charts of the Part I in TC1 with the thicknesses of TC2 as 0 μm, 50 μm, 100 μm, 150 μm, 200 μm and 250 μm. (b) The stress cloud charts of the Part II in TC1 with the thicknesses of TC2 as 0 μm, 50 μm, 100 μm, 150 μm, 200 μm and 250 μm, (c) The stress cloud charts of the Part III in TC1 with the thicknesses of TC2 as 0 μm, 50 μm, 100 μm, 150 μm, 200 μm and 250 μm.

In the finite element model, growth of the oxide layer by external oxidation was modeled by swelling of the elements in the TGO layer in the direction of thickness using the subroutine of USERSW.F in ANSYS to describe the process of TGO growing outward [16]. Comparatively, the growth of the oxide layer by internal oxidation was modeled by "switching" the properties of layers of elements from those of the BC material to those of the TGO to describe the process of TGO growing inward [17–21].

3. Results and discussion

3.1. The behavior of stress buffer effect of the TC2 upon the stress of the TC1

In this section, the stress buffer effect of the TC2 layer, which is made by the material of 8YSZ, was investigated. Rosler [22–23] assumes that the failure of coatings is determined by stresses generated in the room temperature. Based on this, the peeling normal stresses in the thickness direction of the TC1 layer after cooling in a thermal cycle were emphatically investigated to discuss the stress buffer effect of the TC2.

3.1.1. The effect of reducing the stress of TC1

It has been discussed in the first section that the main purpose of introducing the inside ceramic layer in the DCL-TBC is to reduce the high stress level of the top ceramic layer. Fig. 6 shows the stress cloud charts of the TC1 layer in the DCL-TBC in which the thicknesses of TC2 were chosen as 0 μm, 50 μm, 100 μm, 150 μm, 200 μm and 250 μm and the thickness of TC1 was chosen as 150 μm. It has been discussed in Section 2.4 that the DCL-TBC FE model was investigated considering the influence of the edge stress concentration. Based on the FE model and the boundary conditions, three sub-model parts of the TC1 (denoted as Part I, Part II, and Part III), which respectively represent different states of the TC1 layer in the actual DCL-TBC layer, were mainly investigated.

Firstly, it can be seen that the stress distributions in three parts of TC1 are different. At the right edge (Part I), the maximum tensile stress locates at the right edge on top of the TC1/TC2 interface, which reflects the effect of the edge stress concentration, as shown in Fig. 6(a). In the central (Part II), the maximum tensile stress locates at the top left corner of TC1/TC2 interface, which reflects the stress state with partly influenced by the edge stress concentration, as shown in Fig. 6(b). In the left end (Part III), the maximum tensile stress locates at the peak of TC1/TC2 interface and the stress distribution is symmetric, which reflects the stress state with little effect of the edge stress concentration, as shown in Fig. 6 (c).

Secondly, Fig. 7 shows that the maximum tensile stresses of the three parts in the TC1 layer are decreased as the increase in the thickness of the TC2. However, the stress distribution characteristics of the three parts in TC1 shown in Fig. 6 have no change. These results indicate that the stress buffer effect of the TC2 layer has great influence upon the stress level of the top ceramic layer, but the inside ceramic layer has little influence upon the stress distribution and stress generation mechanism of the TC1 layer.

It can be concluded that the TC2 layer, which is made by 8YSZ, has the stress buffer effect on reducing the stress level in TC1, which is the most primary behavior of stress buffer effect of TC2. The stress buffer effect is related to the thickness of the TC2 layer.

3.1.2. The effect of reducing the influence of TGO growth on the stress of TC1

It has been known that the TGO layer is generated and grown due to oxidation of the bond coat at high temperature during the thermal cycling. In the oxidation process, the thickness and internal stress of TGO is increasing. If there is no TC2 layer in the DCL-TBC, the growth of TGO should have great influence on the stress of TC1 as these two layers are adjacent. If the DCL-TBC has the TC2 layer, the two layers of TC1 and TGO are not adjacent, this influence should be affected and related to the thickness of the TC2 layer. So in this section, the influence of the TGO growth after ten thermal cycles upon the stress of TC1 was investigated considering different thicknesses of the TC2 layer. As detailed in Section 2.5.3, the thickness of TGO is growing to 5 μm after ten thermal cycles and the growth stress of TGO is considered, which are all identical and without changing with different thicknesses of the TC2. Calculation results have shown that the growth of TGO has the most influence on the stress of Part I in TC1 compared with the influences on the stresses of Part II and Part III in TC1 as the result of stress concentration in the edge.

Fig. 8 shows the maximum tensile stresses of the Part I in TC1 after one thermal cycle and ten thermal cycles all of which decreased with the increase in the thickness of the TC2. It can be seen that the stress of TC1 after ten cycles (the curve "$\sigma_{N=10}$") is lower than the stress after one cycle (the curve "$\sigma_{N=1}$"). This result illustrates that the growth of TGO has the effect on reducing the stress of TC1. It can also be seen that the two stress curves are gradually close to each other as there is increase in the thickness of TC2. This result denotes that the stress change amplitude $\Delta\sigma$, which is caused by the TGO growth, decreased with the increase in the thickness of TC2. As shown in Fig. 9, the stress change amplitude $\Delta\sigma$ and stress change percentage $\Delta\sigma/\sigma$ all decreased with the increase in the thickness of TC2, which shows that the TC2 layer has the stress buffer effect on reducing the influence of TGO growth on the stress of TC1.

Moreover, some results, which are not detailed in the present paper, show that the stress change amplitude of the TC1 layer, which is caused by change in the TGO interface shape parameter, is also decreased as there is increase in the thickness of the TC2. It can be summarized that the TC2 layer has the stress buffer effect on reducing many kinds of influences upon the stress of TC1 caused by the changes of other layers (such as TGO layer, BC layer and SUB layer), and these influences are wicker as the TC2 is thicker. It can be also concluded that these influences caused from the TGO layer, the BC layer and the SUB layer in the DCL-TBC are gradually

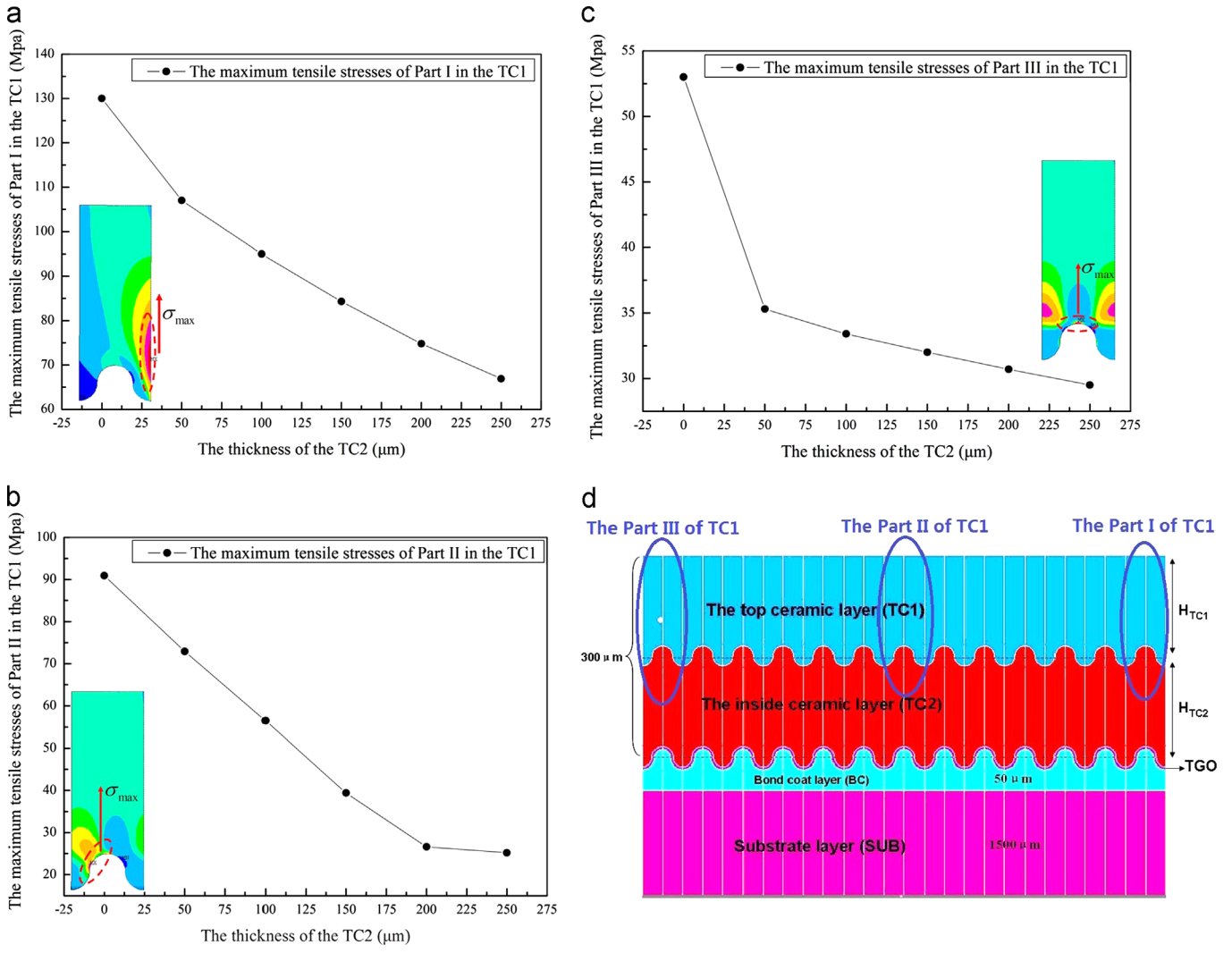

Fig. 7. The schematic view of the maximum tensile stresses in the three different parts as a function of the thickness of the TC2: (a) Part I in TC1, (b) Part II in TC1, (c) Part III in TC1, and (d) schematic view of three parts.

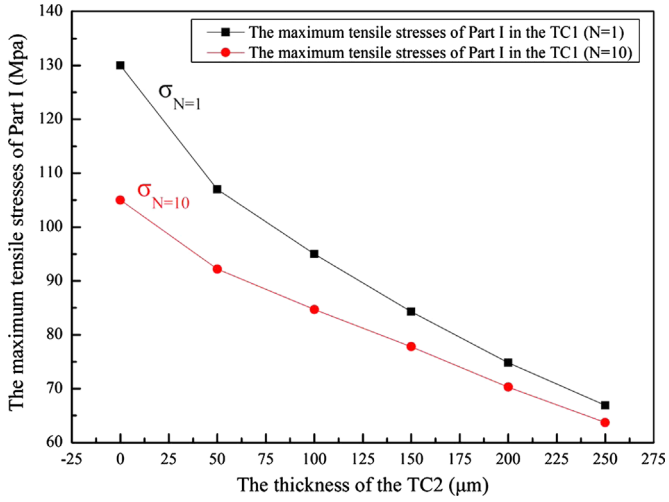

Fig. 8. The schematic view of the maximum tensile stresses of the Part I in TC1, after one thermal cycle and ten thermal cycles, as a function of the thickness of the TC2.

weaker as the distances between these layers and the TC1 layer are increased.

3.2. The internal mechanism of stress buffer effect of the TC2 upon the stress of the TC1

3.2.1. The internal mechanism of stress buffer effect of the TC2 affected by the thermal expansion coefficient ρ

As discussed in Section 3.1.2, the growth of TGO has influence on reducing the stress of TC1 but this influence is limited, such as the DCL-TBC without the TC2 layer, where the stress change amplitude is just 25 Mpa. This stress change amplitude decreases with the increase in the thickness of TC2 and is relatively small compared with the stress level of the TC1. Considering the growth of TGO is a long-term process, it can be concluded that the influence of the TGO growth upon the stress level of TC1 is a very slow process. Based on these, it can also be concluded that other layers in the DCL-TBC, such as BC and SUB which are more away from the TC1

layer, should have little influence on the stress of the TC1 layer.

Based on these analyses above, it can be concluded that the stress of the TC1 layer is mainly determined by the thermal stress caused by the higher degree thermal expansion mismatch with the layers of BC and SUB. The stress buffer effect of the TC2 layer is just aiming at reducing the higher degree thermal expansion mismatch. In that case, the thermal expansion coefficient of the material for the TC2 layer should have much influence upon the stress buffer effect of the TC2 layer.

Fig. 10 shows the variation laws of the maximum tensile stress (denoted as σ_Y) of the three parts in TC1 as a function of thermal expansion coefficient ρ of TC2. The thermal expansion coefficient of 8YSZ (10.4 $^{\circ}C^{-1}$ ($\times 10^{-6}$)), which is widely used as the TC2 layer, and the thermal expansion coefficient of LZ_7C_3 (9.1 $^{\circ}C^{-1}$ ($\times 10^{-6}$)), which is widely used as the TC1 layer, are all marked in Fig. 10.

The results show several tendencies for the stress evolution in TC1 studied:

(1) In the range of $\rho_{TC2} > \rho_{LZ_7C_3}$, the σ_Y of the Part I in TC1 increases linearly as the ρ of TC2 increases, which shows that the rise of the ρ_{TC2} has the effect of relieving the stress concentration in the edge. However, the σ_Y variation laws of the Part II and Part III are not linear. As the ρ of TC2 increases, the σ_Y of Part II and Part III decrease first then increase. It shows that the stress buffer effect of TC2 is enhanced as the ρ_{TC2} is increased in the initial stage. If the ρ_{TC2} is large enough, the stress of TC1 increases with the increase in ρ_{TC2}. The reason is that the thermal mismatch expansion between the TC1 and TC2 becomes higher, which causes the stress of the TC1 increased and the stress buffer effect of TC2 reduced. The Part II and Part III of the TC1 layer have the lowest stresses at the points of $\rho_{TC2}=10.6$ and $\rho_{TC2}=9.8$.

(2) In the range of $\rho_{TC2} > \rho_{LZ_7C_3}$, the σ_Y of the Part I, Part II and Part III all increased as the ρ of TC2 decreased. The characteristic of stress distribution in TC1 has changed as the ρ of TC2 is lower than the ρ of TC1 (LZ_7C_3) which is 9.1. In this situation, the TC2 do not have the stress buffer effect to reduce the stress of TC1.

It can be summarized that the thermal expansion coefficient ρ of TC2, which has a dominant influence on the stress buffer effect of TC2, should be neither too high nor too low. If the thermal expansion coefficient of TC2 is too low, the stress buffer effect is insufficient to reduce the stress of TC1. If the TC2 has a higher thermal expansion coefficient, the stress of TC1 is still high which is caused by the thermal expansion mismatch between the TC1 and the TC2. In this situation, the stress buffer effect is gradually reduced and lost. These two shortcomings of the thermal expansion coefficient ρ of TC2 are presented in Fig. 11.

3.2.2. The discussion of the thermal expansion coefficient reasonable range

The internal mechanism of stress buffer effect of the TC2 mainly originates from reducing the high degree thermal

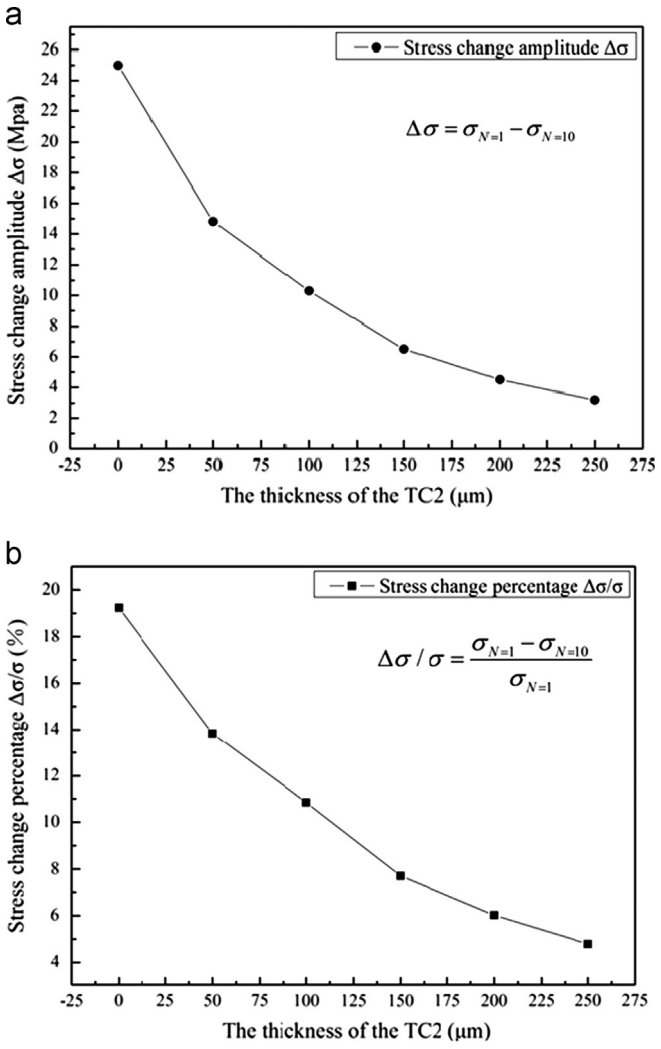

Fig. 9. The schematic view of the influence of the TGO growth upon the maximum tensile stresses of the Part I in TC1 as a function of the thickness of TC2: (a) the stress change amplitude $\Delta\sigma$ and (b) the stress change percentage $\Delta\sigma/\sigma$.

expansion mismatch between the TC1 and the layers of SUB and BC. It is not suitable for all the TBC materials to be chosen for producing the inside ceramic layer [1,22–25]; the TC2 layer should have reasonable thermal expansion coefficient, in which condition the stress of TC1 can be reduced to a "safe stage" and the stress buffer effect is effective.

In the present study, the investigation work of the reasonable range of the thermal expansion coefficient is also aimed at the DCL-TBC in which the thicknesses of two ceramic layers are all 150 μm. It should be mentioned that the reasonable range of the thermal expansion coefficient is different as the two ceramic layers have different thickness ratios. So the main purpose of our work is to provide a method of investigating the reasonable range of the thermal expansion coefficient.

It has been discussed that the inside ceramic layer with reasonable thermal expansion coefficient should ensure the stress of TC1 is in a safe range during the thermal cycles. To investigate this "safe range", the steady state cracking criteria proposed by A.G.Evans and J.W.Hutchinson was used [26–28]. The energy available for delamination is expressed though

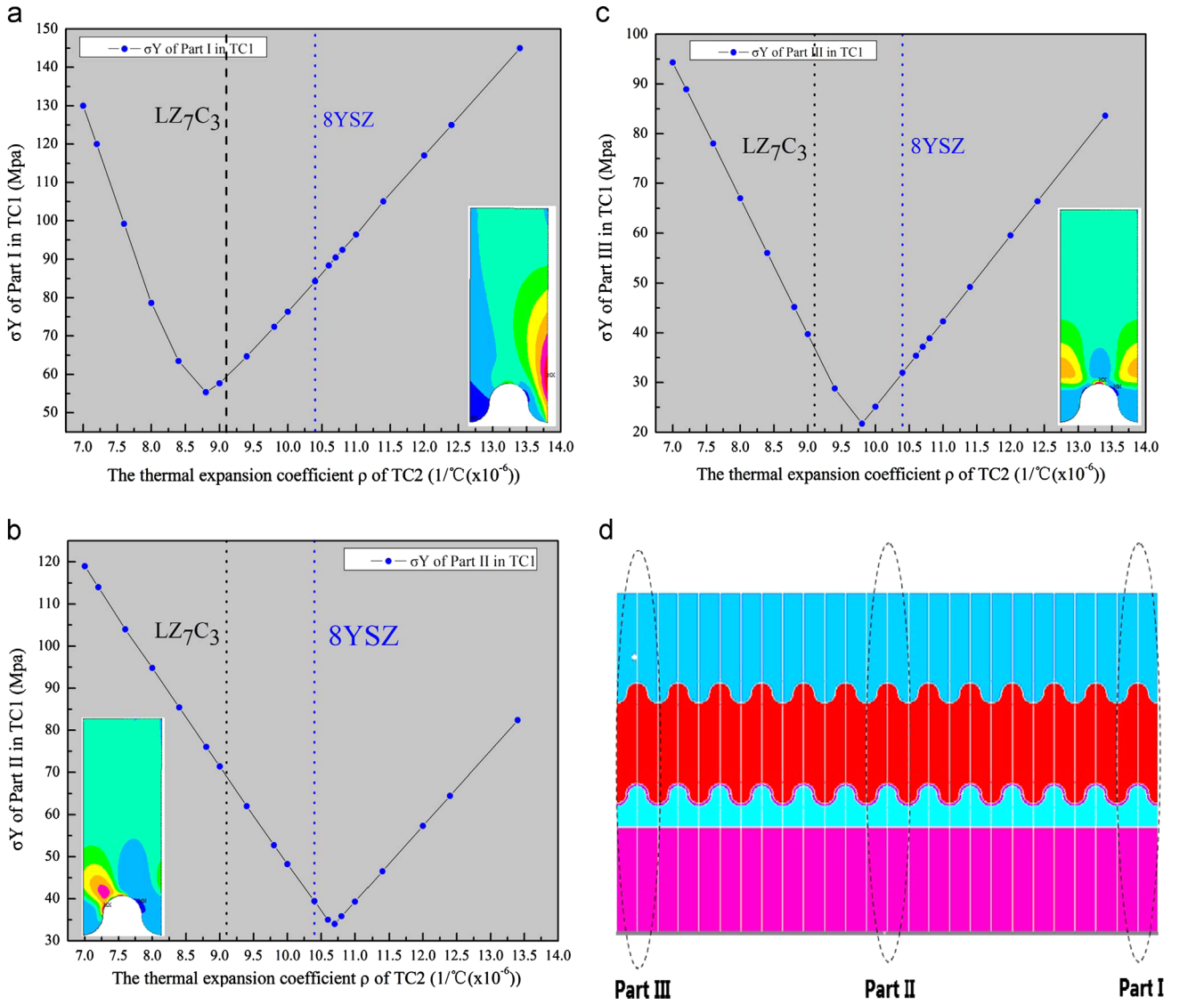

Fig. 10. The stress σ_Y of the three parts in TC1, after cooling in one cycle, as a function of thermal expansion coefficient ρ of TC2: (a) Part I of the TC1, (b) Part II of the TC1, (c) Part III of the TC1 and (d) schematic view of three parts.

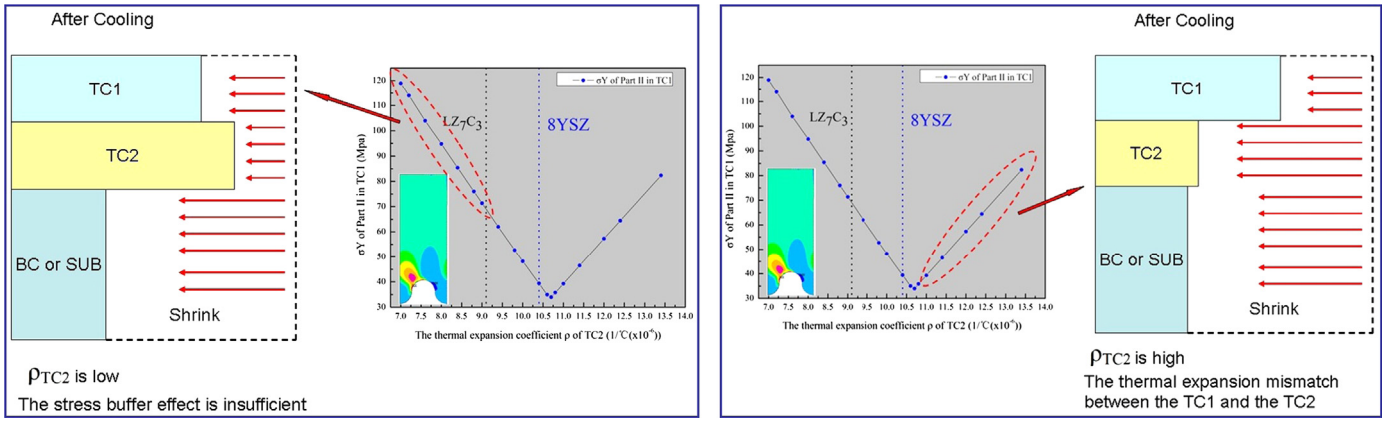

Fig. 11. The schematic view of the explanation of the increase in stress in the two conditions that the thermal expansion coefficient is lower and the thermal expansion coefficient is higher.

the steady-state energy release rate [29].

$$G_{SS} = \frac{(1-\upsilon^2)}{2E}\sigma_0 h \tag{4}$$

with E and ν as Young's modulus and Poisson's ratio of the layer, respectively and h as the thickness of the layer. A.G. Evans assumes that, if $G_{ss} > G_{IC}$, where G_{IC} is the toughness, delamination will be expected to occur in the layer, and the layer is not in "safe state"; if $G_{ss} < G_{IC}$, delamination will not be expected to occur, the layer is in "safe state" [27].

Specifically, the safety criterion of the TC1 was presented referred the steady state cracking criteria:

(1) If $G_{ss} > G_{IC}$, the TC1 is "unsafe".
(2) If $G_{ss} \leq G_{IC}$, the TC1 is "safe".

Specifically, at the critical state $G_{ss}=G_{IC}$, it was accounted that the TC1 is "safe" in our study. The reason is that the steady state cracking criteria is a conservative criterion.

In our study, for the TC1 layer made by LZ_7C_3, the fracture toughness K_{IC} is 0.35 Mpa $m^{1/2}$ based on experiment. According to the transfer formula (5), $G_{IC}=0.672$ J m^{-2}.

$$G_{IC} = \frac{(1-\upsilon^2)K_{IC}}{E} \tag{5}$$

In the earlier work, it had been discussed that the maximum tensile stress in Y direction after one thermal cycle has a dominant influence upon the cracking failure of TC1. Consequently, σ_Y of the TC1 layer, after one thermal cycle, was chosen to calculate the G_{ss}, as shown in Fig. 12.

It must be mentioned that the stress of Part I in the TC1 was not chosen to determine whether the TC1 is a failure in our present study. The reason can be explained from two aspects. Firstly, the cracking at the edge cannot determinate the cracking failure of the whole TC1, as the compressive stress region, which is ahead next to the stress concentration region, prevents the crack from propagating to the internal of TC1. On the other hand, the high tensile stress range affected by the edge stress concentration is too narrow (<30 μm) to influence the cracking failure and life expectancy level of the whole DCL-TBC. Secondly, in airplane engine blades, the edge of the coatings should be avoided for the stress concentration, usually through the method of chamfering the edge or coating the edge surface, which relives the concentrated stress level but has limited influence on the stress of the inner coatings. For these reasons, the stresses of Part II and Part III in the TC1, which can represent the real stress state of the DCL-TBC under the service condition, were investigated emphatically.

Fig. 13 presents the G_{ss} of Part II and Part III in the TC1 influenced by the material property ρ of the TC2. The safety criterion $GIC=0.672$ J m^{-2} is marked using the red line, and the intersection points of the two curves shown in Fig. 13 present the boundary points of the reasonable range of the thermal expansion coefficient of the "TC2 layer", and the "the TC2 layer" is missing at the end of the sentence.

As shown in Fig. 13(a), if the stress level of Part II in TC1 is in the safe range, the thermal expansion coefficient ρ of TC2 should be selected between the value of 10.35 $°C^{-1}$ ($\times 10^{-6}$) and the value of 11.05 $°C^{-1}$ ($\times 10^{-6}$); the reasonable range of the ρ of TC2 determined by the stress of Part II in TC1 is from 10.35 to 11.05. As shown in Fig. 13(b), if the stress level of Part III in TC1 is in the safe range, the thermal expansion coefficient ρ of TC2 should be selected smaller than the value of 10.887 $°C^{-1}$ ($\times 10^{-6}$); the reasonable range of the ρ of TC2 determined by the stress of Part III in TC1 is from the lowest investigated value to 10.887.

In our study, it has been determined that the whole TC1 is in safe state only if the material property ρ simultaneously locates in the two reasonable ranges. It can be obtained if the intersection range of the two reasonable ranges is from 10.35 $°C^{-1}$ ($\times 10^{-6}$) to 10.887 $°C^{-1}$ ($\times 10^{-6}$). If the inside ceramic layer has the thermal expansion coefficient ρ in this range, the stress buffer effect of the TC2 layer is effective.

As an important conclusion, it should be mentioned that this result shows that the material of 8YSZ is just a good material for the inside ceramic layer in the DCL-TBC, as the thermal expansion coefficient of 8YSZ, which is 10.4 $°C^{-1}$ ($\times 10^{-6}$), just locates in the reasonable range. As shown in the calculation results (Fig. 10 or Fig. 13), if the material parameters of the TC2 layer is chosen same as that of the material 8YSZ, the TC1 layer has a lower stress level. Meanwhile, it had been well known that the DCL-TBC (the two ceramic layers thickness ratio as 150 μm–150 μm), which has the inside ceramic layer as the 8YSZ, is widely used and has good

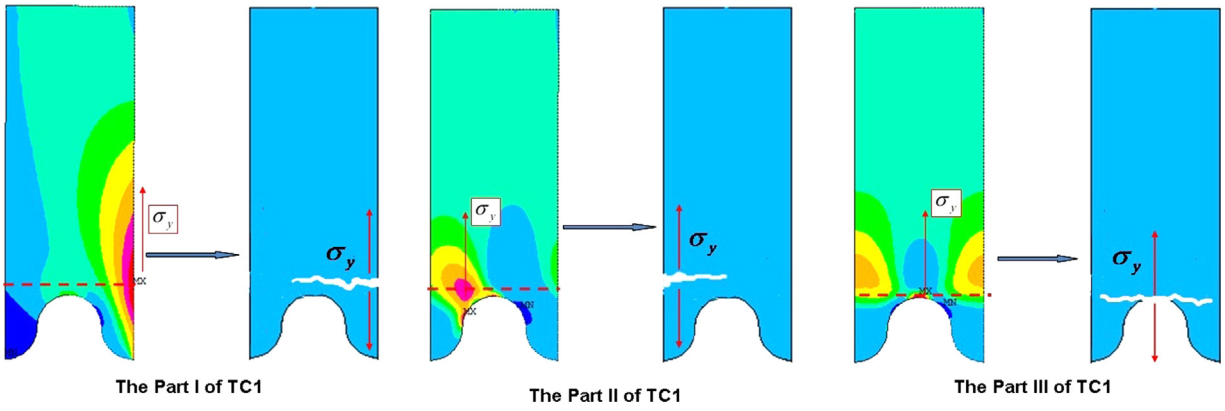

Fig. 12. Schematic view of cracking failure of TC1 dominant influenced by the maximum tensile stress in Y direction.

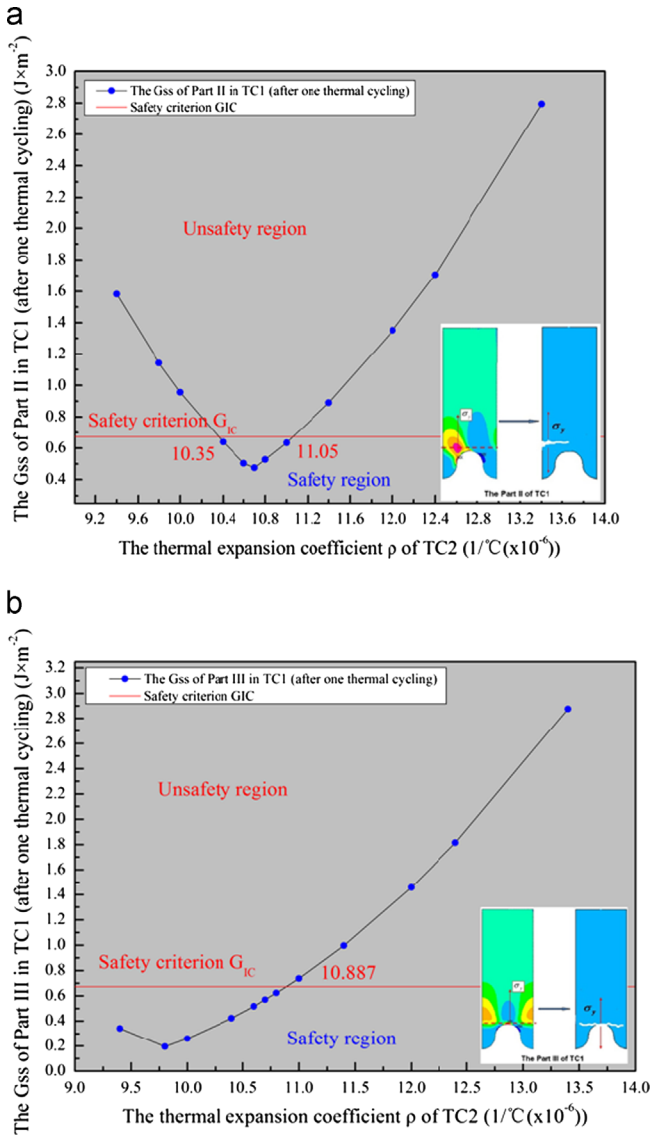

Fig. 13. The G_{ss} of Part II and Part III in the TC1 as a function of the thermal expansion coefficient ρ of TC2: (a) the G_{ss} of Part II in TC1 and (b) The G_{ss} of Part III in TC1.

thermal cycling performance based upon a lot of experiment results [4]. As reported by Cao, during the thermal cycling experiment of the DCL-TBC(150 μm-150 μm, LZ_7C_3-8YSZ), the cracking failure finally occurred in the TGO layer and the TC1 layer was safe. According to these experiment phenomenas, it can be concluded that the stress level of the TC1 layer is reduced to a safe state by choosing the 8YSZ as the TC2 layer, which agrees well with the calculation results of our study. The thermal expansion coefficient reasonable range obtained in our study has proven the rationality of selecting the 8YSZ as the inside ceramic layer in the DCL-TBC through the theoretical calculation.

4. Conclusions

In this work, a DCL-TBC FE model was presented. The stress of the top ceramic layer in the DCL-TBC during the thermal cycling was calculated using the FE numerical simulation. The main purpose of the present work is to investigate the stress buffer effect of the inside ceramic layer upon the stress of the top ceramic layer in the DCL-TBC.

In the first part of the present paper, the behavior of the stress buffer effect of the TC2 layer was investigated based on the influence of the thickness of the TC2 layer upon the stress level of TC1. Results have shown that the TC2 layer has the effect of reducing the higher stress level of the TC1 layer, and the stress of TC1 decreases as the thickness of TC2 is increased. It can be summarized that the stress buffer effect firstly manifests as the effect of reducing the stress level of TC1. Furthermore, the introduction of the TC2 layer has affected the influence of the TGO growth upon the stress of TC1. Results have shown that the TGO growth has the effect of reducing the stress of TC1, and the stress reduction amplitude decreases with the increase in the thickness of TC2. This conclusion can be summarized by saying that the TC2 layer has stress buffer effect on weakening and shielding the influence of the TGO growth upon the stress of TC1.

In the second part of the present paper, the internal mechanism of stress buffer effect was investigated based on studying the influence of the thermal expansion coefficient ρ upon the stress of TC1. Results show that the stress of the TC1 layer is determined by the thermal stress which is mainly caused by the thermal expansion mismatch with the layers of BC and SUB, and the stress buffer effect of the TC2 layer can reduce this mismatch. The stresses of TC1 are different if the TC2 layer has different thermal expansion coefficients. The thermal expansion coefficient ρ of TC2, which has a dominant influence on the stress buffer effect of TC2, should be neither too high nor too low. If the thermal expansion coefficient of TC2 is too low, the stress buffer effect is insufficient to reduce the stress of TC1. The stress of TC1 is decreased and the stress buffer effect is enhanced with the increase in the thermal expansion mismatch of TC2. Meanwhile, if the TC2 has a larger thermal expansion coefficient, the stress of TC1 is still high, which is caused by the thermal expansion mismatch between the TC1 and the TC2. In this situation, the stress buffer effect is reduced or lost. Based on the two kinds of influences of the thermal expansion coefficient of TC2, the reasonable range of the thermal expansion coefficient of TC2 was investigated. The TC2 layer with thermal expansion coefficient in this reasonable range should ensure the stress level of TC1 in the safe state and the stress buffer effect is effective. Aiming at the DCL-TBC with the thicknesses of the two ceramic layer as 150 μm, the reasonable range of the thermal expansion coefficient of TC2 had been obtained, which is from $10.35\ ^\circ C^{-1}$ $(\times 10^{-6})$ to $10.887\ ^\circ C^{-1}$ $(\times 10^{-6})$. The results of the present work have important guiding meanings in material selection and developing new materials for the inside ceramic layer in the DCL-TBC.

It should be mentioned that the investigation of the thermal expansion coefficient reasonable range in our present work was mainly aimed at the DCL-TBC in which the thicknesses of two ceramic layers are both150 μm. Our present work was aimed at providing the method of exploring the thermal expansion coefficient reasonable range of the TC2 layer in

the DCL-TBC. The reasonable range of the thermal expansion coefficient the TC2 layer in the DCL-TBC with the two ceramic layer thicknesses as different values can be studied using same method and is not detailed in the present paper.

Acknowledgments

This work is supported by the National Key Development Program for Fundamental Research under the Contract 61311203B.

References

[1] X.Q. Cao, R. Vassen, D. Stoever, Ceramic materials for thermal barrier coatings, J. Eur. Ceram. Soc. 24 (1) (2004) 1–10.
[2] X.Q. Cao, Application of rare earths in thermal barrier coating materials, J. Mater. Sci. Technol. 23 (1) (2007) 15–35.
[3] H. Dai, X.H. ZHONG, X.Q. CAO, Thermal stability of double-ceramic-layer thermal barrier coatings with various coating thickness, Mater. Sci. Eng. A433 (2006) 1–7.
[4] Z.H. Xu, L.M. He, X.Q. Cao, Double-ceramic-layer thermal barrier coatings of La2Zr2O7/YSZ deposited by electron beam-physical vapor deposition, J. Alloys Compd. 473 (2009) 509–515.
[5] M. Białas, Finite element analysis of stress distribution in thermal barrier coatings, Surf. Coat. Technol. 202 (2008) 6002–6010.
[6] P. Bednarz, Finite element simulation of stress evolution in thermal barrier coating systems, Ph.D. Thesis, Forschungszntrum Jülich, Germany, 2007.
[7] K. Sfar, J. Aktaa, D. Munz, Numerical investigation of residual stress fields and crack behavior in TBC systems, Mater. Sci. Eng. A333 (2002) 351–360.
[8] J. Aktaa, K. Sfar, D. Munz, Assessment of TBC systems failure mechanisms using a fracture mechanics approach, Acta Mater. 53 (2005) 4399–4413.
[9] E.P. Busso, L. Wright, H.E. Evans, et al., A physics-based life prediction methodology for thermal barrier coating systems, Acta Mater. 55 (2007) 1491–1503.
[10] V. Teixeira, Analysis of residual stresses in thermal barrier coatings, J. Mater. Process. Technol. 92–93 (30) (1999) 209–216.
[11] J. Rosler, M. Baker, K. Aufzug, A parametric study of the stress state of thermal barrier coatings Part I: creep relaxation, Acta Mater. 52 (2004) 4809–4817.
[12] U. Hermosilla, M.S. Karunaratne, I.A. Jones, Modelling the high temperature behaviour of TBCs using sequentially coupled microstructural–mechanical FE analyses, Mater. Sci. Eng. A513 (2009) 302–310.
[13] E.P. Busso, Z.Q. Qian, M.P. Taylor, et al., The influence of bondcoat and topcoat mechanical properties on stress development in thermal barrier coating systems, Acta Mater. 57 (2009) 2349–2361.
[14] E.P. Busso, J. Lin, S. Sakural, et al., A mechanistic study of oxidation-induced degradation in a plasma-sprayed thermal barrier coating system part I: model formulation, Acta Mater. 49 (2001) 1515–1528.
[15] E.P. Busso, J. Lin, S. Sakural, et al., A mechanistic study of oxidation-induced degradation in a plasma-sprayed thermal barrier coating system part II: life prediction model, Acta Mater. 49 (2001) 1529–1536.
[16] ANSYS Release 10.0, Guide to ANSYS User Programmable Features, 2009.
[17] U. Hermosilla, University of Nottingham, England, 2008 ([Ph.D. thesis]).
[18] D.R. Clarke, Critical radius for interface separation of a compressively stressed film from a rough surface, Acta Mater. 47 (1999) 1749–1756.
[19] V.K. Tolpygo, D.R. Clarke, K.S. Murphy, Oxidation-induced failure of EB-PVD thermal barrier coatings, Surf. Coat. Technol. 146 (2001) 124–131.
[20] A.G. Evans, D.R. Clarke, C.G. Levi, The influence of oxides on the performance of advanced gas turbines, J. Eur. Ceram. Soc. 28 (2008) 1405–1419.
[21] V.K. Tolpygo, J.R. Dryden, D.R. Clarke, Determination of the growth stress and strain in α-Al_2O_3 scales during the oxidation of Fe-22Cr–4.8Al–0.3Y alloy, Acta Mater. 46 (1998) 927–937.
[22] M. Baker, J. Rosler, G. Heinze, A parametric study of the stress state of thermal barrier coatings. Part II: cooling stresses, Acta Mater. 53 (2005) 469–476.
[23] E.P. Busso, L. Wright, H E Evans, et al., A physics-based life prediction methodology for thermal barrier coating systems, Acta Mater. 55 (2007) 1491–1503.
[24] H. Dai, X.H. Zhong, X.Q. Cao, Thermal stability of double-ceramic-layer thermal barrier coatings with various coating thickness, Mater. Sci. Eng. A433 (2006) 1–7.
[25] X.Q. Cao, R. Vassen, W. Jungen, Thermal stability of lanthanum zirconate plasma-sprayed coating, J. Am. Ceram. Soc. 84 (9) (2001) 2086–2090.
[26] A.G. Evans, Mechanisms controlling the durability of thermal barrier coatings, Prog. Mater. Sci. 46 (2001) 505–553.
[27] M.Y. He, D.R. Mumm, A.G. Evans, Criteria for the delamination of thermal barrier coatings: with application to thermal gradients, Surf. Coat. Technol. 185 (2004) 184–193.
[28] H.H. YU, M.Y. He, J.W. Hutchinson, Edge effects in thin film delamination, Acta Mater. 49 (2001) 97–107.
[29] V.K. Tolpygo, D.R. Clarke, Alumina scale failure resulting from stress relaxation, Acta Mater. 47 (1999) 3589–3605.